

H1-prelim-14-071, ZEUS-prel-14-006
April 24, 2014

Determination of Charm Mass Running from an Analysis of Combined HERA Charm Data

The H1 and ZEUS Collaborations,
and S. Moch (Hamburg University)

Abstract

The combined HERA data on charm production in deep inelastic scattering have recently been used to determine the charm quark running mass $m_c(m_c)$ in the $\overline{\text{MS}}$ renormalisation scheme. The same data are used differentially as a function of the photon virtuality Q^2 to evaluate the charm quark running mass at different scales to one-loop order. The scale dependence of the mass is found to be consistent with QCD expectations, and a graphical representation of the charm mass running, similar to the representation of the beauty mass running from LEP data, is obtained from data for the first time.

1 Introduction

In the $\overline{\text{MS}}$ scheme of perturbative quantum chromodynamics (pQCD), the values of all basic QCD parameters depend on the scale at which they are evaluated. The scale dependence ('running') of the strong coupling constant α_s has first been established from jet production at e^+e^- colliders such as the PETRA collider at DESY [1] and is by now a very well tested property of QCD which can also be extracted from jet production at HERA [2], Tevatron [3] or LHC [4].

The scale dependence of the masses of heavy quarks can likewise be evaluated perturbatively. The running of the $\overline{\text{MS}}$ beauty quark mass has been established from measurements at the LEP e^+e^- collider [5]. An explicit determination of the running of the charm quark mass had not yet been performed so far. Here, we will use the combined HERA data [6] on charm production in deep inelastic scattering (DIS) (Fig. 1) to extract such a determination. These data have recently been used for several determinations of the charm quark running mass $m_c(m_c)$ in the $\overline{\text{MS}}$ renormalisation scheme [6, 7].

2 Principle of the measurement

The principle of this measurement is the following. The reduced cross section for charm production is obtained from a convolution of charm production matrix elements with appropriate parton density functions (PDF). Both of these depend on the value of the charm quark mass and on other theoretical and phenomenological parameters. A set of PDFs in the fixed flavour number scheme (FFNS) is extracted from inclusive DIS HERA data [8] using exactly the same setup as the one used in a previous publication [6], but varying the charm mass. For each charm quark mass hypothesis, predictions for the reduced charm cross section are obtained using the corresponding PDF and are compared to corresponding charm data [6]. The χ^2 distribution of this comparison (Fig. 2) is used to extract the value of the charm quark mass $m_c(m_c)$. In contrast to earlier determinations, the charm data are subdivided into several kinematic intervals according to the virtuality of the exchanged photon (Table 1 and Fig. 1). A value of $m_c(m_c)$ is extracted separately for each interval (Fig. 3). As to be expected from Fig. 1, the data are always well described. The $m_c(m_c)$ value is obtained assuming the running of both α_s and m_c as predicted by QCD. However, each measurement is performed with data originating from collisions at a typical scale of $\mu = \sqrt{Q^2 + 4m_c^2}$. Thus, if each measurement is reinterpreted in terms of a value of $m_c(\mu)$ at this scale (Fig. 4), the effect of the initial assumption of QCD running on the interpretation of the measurement is minimised. The comparison of $m_c(\mu)$ at different scales with the expected running behaviour (Fig. 4) yields a nontrivial consistency check of the charm mass running. This method is conceptually similar to the procedure of extracting the running of $\alpha_s(\mu)$ from jet production at different transverse energy scales or at different e^+e^- centre-of-mass energies.

3 Theory

QCD predictions for the reduced charm cross sections were obtained at next-to-leading order (NLO) in pQCD ($O(\alpha_s^2)$) using the OPENQCDRAD package [9] as available in HERAFitter [8, 10], which is based on the ABM implementation [11] of charm calculations in the 3-flavour

FFNS scheme. The calculations used the same settings and parametrisations as those used for the earlier measurement of $m_c(m_c)$ [6]. In addition, scale variations were applied as in [7]. For all explicit charm mass running calculations the one-loop formula [12] is used, which is consistent with the one used implicitly in OPENQCDRAD.

As a result, the following parameters and their variations are thus used in the calculations

- **$\overline{\text{MS}}$ running mass of the charm quark**, varied within the range $m_c(m_c) = 1 \text{ GeV}$ to $m_c(m_c) = 1.5 \text{ GeV}$ in several steps (Fig. 2);
- **strong coupling constant** $\alpha_s^{n_f=3}(M_Z) = 0.105 \pm 0.002$, corresponding to $\alpha_s^{n_f=5}(M_Z) = 0.116 \pm 0.002$;
- **the proton structure** is described by a series of FFNS variants of the HERAPDF1.0 set [8] at NLO, evaluated for the respective charm mass, for $\alpha_s^{n_f=3}(M_Z) = 0.105 \pm 0.002$. Charm measurements are not included in these fits, such that the effect of the choice of the charm mass is small. The PDF uncertainties are calculated according to the HERAPDF1.0 prescription [8].
- **renormalisation and factorisation scales** $\mu_f = \mu_r = \sqrt{Q^2 + 4m_c(m_c)^2}$, varied simultaneously up or down by a factor of two.

4 Discussion and conclusions

The running of the charm mass $m_c(\mu)$ in the $\overline{\text{MS}}$ scheme (Fig. 4) is measured for the first time from the combined HERA charm reduced cross section data, and found to be consistent with expectations from QCD. Within the limited scale range of each subset of the charm data used for the measurement of $m_c(\mu)$, the charm mass running is implicitly assumed as part of the QCD theory input. Therefore this measurement is not fully unbiased. However, the implicit bias of each individual $m_c(\mu)$ value is much smaller than the one of the earlier extractions of a single $m_c(m_c)$ value [6, 7] from the complete data set. Furthermore, the PDG [13] value of $m_c(m_c)$ indicated in Figs. 3 and 4 is mainly obtained from lattice gauge theory and time-like processes at scales in the vicinity of the charm quark mass at which its value is displayed. Therefore this is an important consistency check, similar in spirit to earlier evaluations of the running of m_b [5] or of the running of α_s [1–4].

Acknowledgements

Part of this work was carried out within the scope of the PROSA collaboration.

References

- [1] O. Biebel, “Experimental tests of the strong interaction and its energy dependence in electron positron annihilation”, Phys. Rept. 340 (2001) 165-289; and references therein. J. Schieck *et al.* [JADE Collaboration], “Measurement of the strong coupling α_S from the three-jet rate in e+e- annihilation using JADE data”, Eur. Phys. J. C73 (2013) 2332 [arXiv:1205.3714].

- [2] F.D. Aaron *et al.* [H1 Collaboration], “Jet Production in ep Collisions at High Q^{*2} and Determination of $\alpha(s)$ ”, Eur. Phys. J. C65 (2010) 363 [arXiv:0904.3870].
 F.D. Aaron *et al.* [H1 Collaboration], “Jet Production in ep Collisions at Low Q^{*2} and Determination of $\alpha(s)$ ”, Eur. Phys. J. C67 (2010) 1 [arXiv:0911.5678].
 H. Abramowicz *et al.* [ZEUS Collaboration], “Inclusive-jet photoproduction at HERA and determination of $\alpha(s)$ ”, Nucl.Phys. B864 (2012) 1 [arXiv:1205.6153].
- [3] V.M. Abazov *et al.* [D0 Collaboration], “Determination of the strong coupling constant from the inclusive jet cross section in $p\bar{p}$ collisions at $\sqrt{s}=1.96$ TeV”, Phys. Rev. D80 (2009) 111107 [arXiv:0911.2710].
 V.M. Abazov *et al.* [D0 Collaboration], “Measurement of angular correlations of jets at $\sqrt{s} = 1.96$ TeV and determination of the strong coupling at high momentum transfers”, Phys. Lett. B718 (2012) 56-63 [arXiv:1207.4957].
- [4] S. Chatrchyan *et al.* [CMS Collaboration], “Measurement of the ratio of the inclusive 3-jet cross section to the inclusive 2-jet cross section in pp collisions at $\sqrt{s} = 7$ TeV and first determination of the strong coupling constant in the TeV range”, Eur. Phys. J. C73 (2013) 2604 [arXiv:1304.7498].
- [5] J. Abdallah *et al.* [DELPHI Collaboration], “Study of b-quark mass effects in multijet topologies with the DELPHI detector at LEP”, Eur. Phys. J. C 55 (2008) 525.
- [6] F.D. Aaron *et al.* [H1 and ZEUS Collaborations], “Combination and QCD Analysis of Charm Production Cross Section Measurements in Deep-Inelastic ep Scattering at HERA”, Eur. Phys. J. C73 (2013) 2311 [arXiv:1211.1182], and references therein.
- [7] S. Alekhin *et al.*, “Precise charm-quark mass from deep-inelastic scattering”, Phys. Lett. B 720 (2013), 172.
- [8] F. D. Aaron *et al.* [H1 and ZEUS Collaboration], “Combined Measurement and QCD Analysis of the Inclusive $e^+ p$ Scattering Cross Sections at HERA,” JHEP 1001, (2010) 109 [arXiv:0911.0884].
- [9] S. Alekhin, “OPENQCDRAD-1.5”,
<http://www-zeuthen.desy.de/~alekhin/OPENQCDRAD>.
- [10] HERAFitter, <http://herafitter.org>.
 M. Botje, “Fast QCD evolution and convolution”, Comput. Phys. Commun. 182 (2011) 490.
 F. James, M. Roos, Comput. Phys. Commun. 10 (1975) 343.
- [11] S. Alekhin, J. Blümlein, S. Klein and S. Moch, “The 3, 4, and 5-flavor NNLO Parton from Deep-Inelastic-Scattering Data and at Hadron Colliders”, Phys. Rev. D 81 (2010) 014032 [arXiv:0908.2766].
 S. Alekhin, S. Moch, “Running Heavy-Quark Masses in DIS”, arXiv:1107.0469.
- [12] B. Schmidt, M. Steinhauser, “CRunDec: a C++ package for running and decoupling of the strong coupling and quark masses”, arXiv:1201.6149 [hep-ph].
 K.G. Chetyrkin, J.H. Kühn, M. Steinhauser, “RunDec: a Mathematica package for running and decoupling of the strong coupling and quark masses”, Comput. Phys. Commun. 133 (2000) 43.
- [13] J. Beringer *et al.* [Particle Data Group], Phys. Rev. D86 (2012) 1.

interval	Q^2 range [GeV ²]
1	2.5-7
2	12-18
3	32-60
4	120-200
5	350-650
6	2000

Table 1: Q^2 intervals used for the measurement of $m_c(\mu)$ with $\mu = \sqrt{Q^2 + 4m_c(m_c)^2}$. The intervals have been chosen to be roughly equidistant in $\log \mu$. The first Q^2 interval is larger than the others since the $4m_c(m_c)^2$ term dominates.

H1 and ZEUS

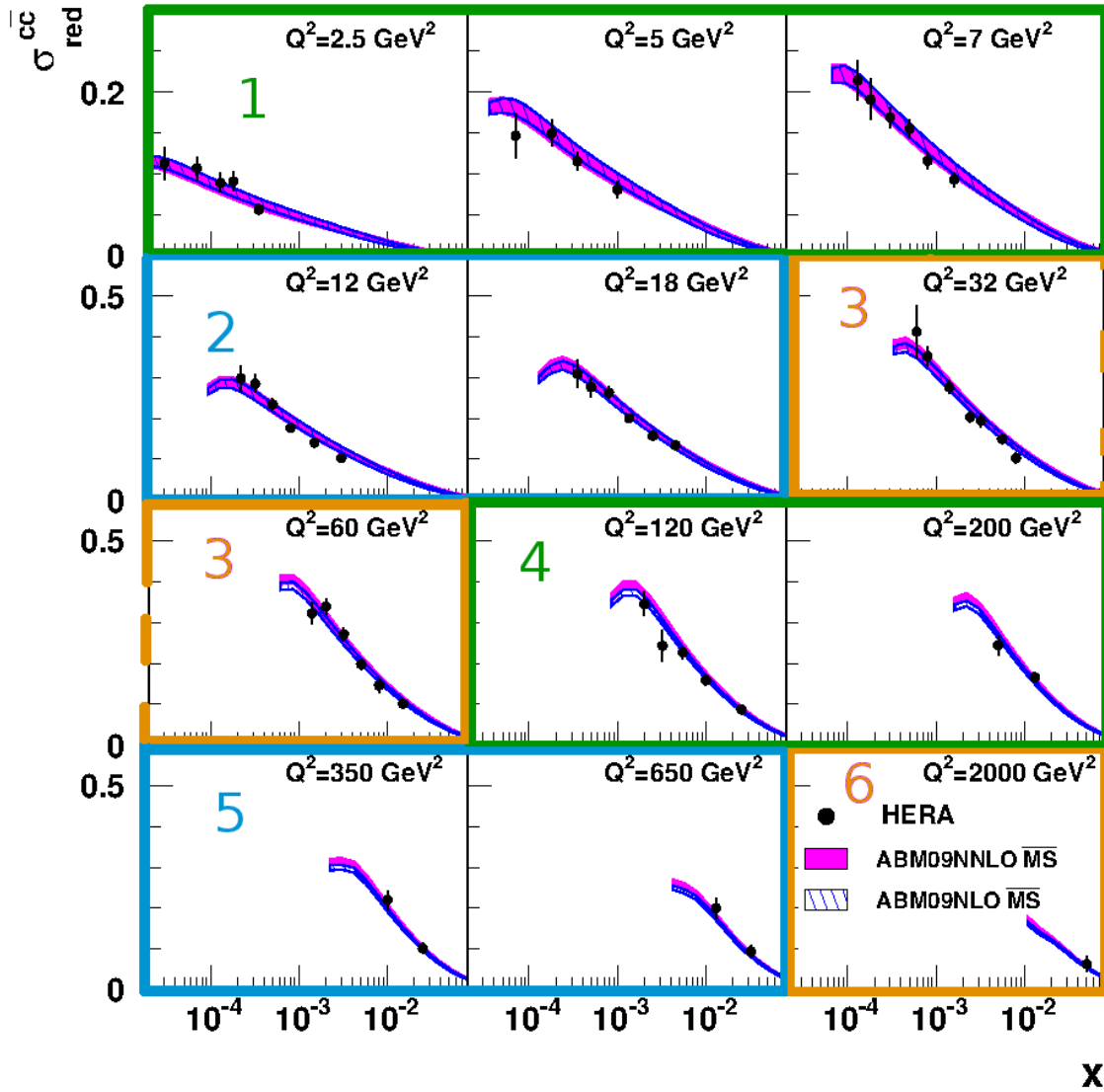


Figure 1: Reduced cross section for charm production in deep inelastic scattering [6] as a function of the Bjorken scaling variable x for different values of photon virtuality Q^2 (points). Also shown are NLO and approximate NNLO QCD predictions [11] (bands) using the $\overline{\text{MS}}$ running mass scheme. They describe the data well. The measurements are grouped into six subsets in Q^2 , as indicated by the numbers and thick boxes, and detailed in Table 1.

H1 and ZEUS preliminary

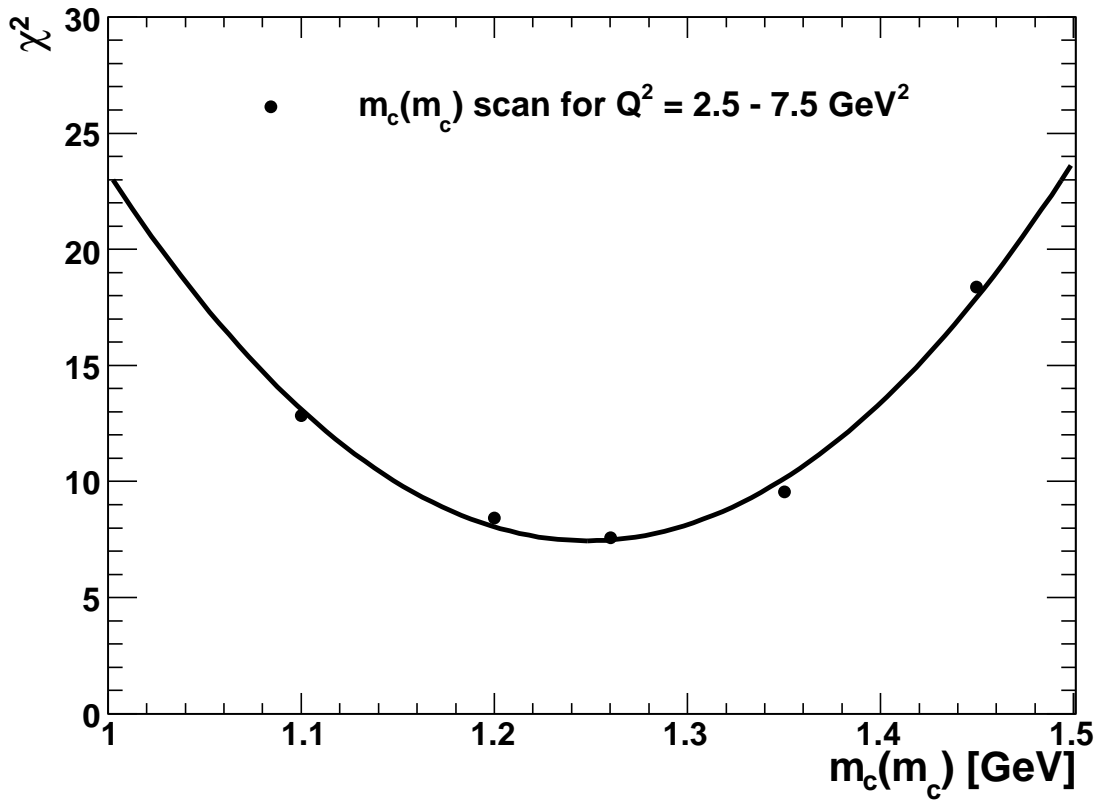


Figure 2: χ^2 of the comparison of the FFNS NLO QCD prediction to the charm reduced cross sections in the first Q^2 interval, 2.5-7 GeV², of Fig. 1, for different values of the charm quark mass $m_c(m_c)$ in the $\overline{\text{MS}}$ running mass scheme (points). The line shows a parabolic fit to the points. The minimum yields the measured charm mass, while the fit uncertainty is obtained from $\Delta\chi^2 = 1$.

H1 and ZEUS preliminary

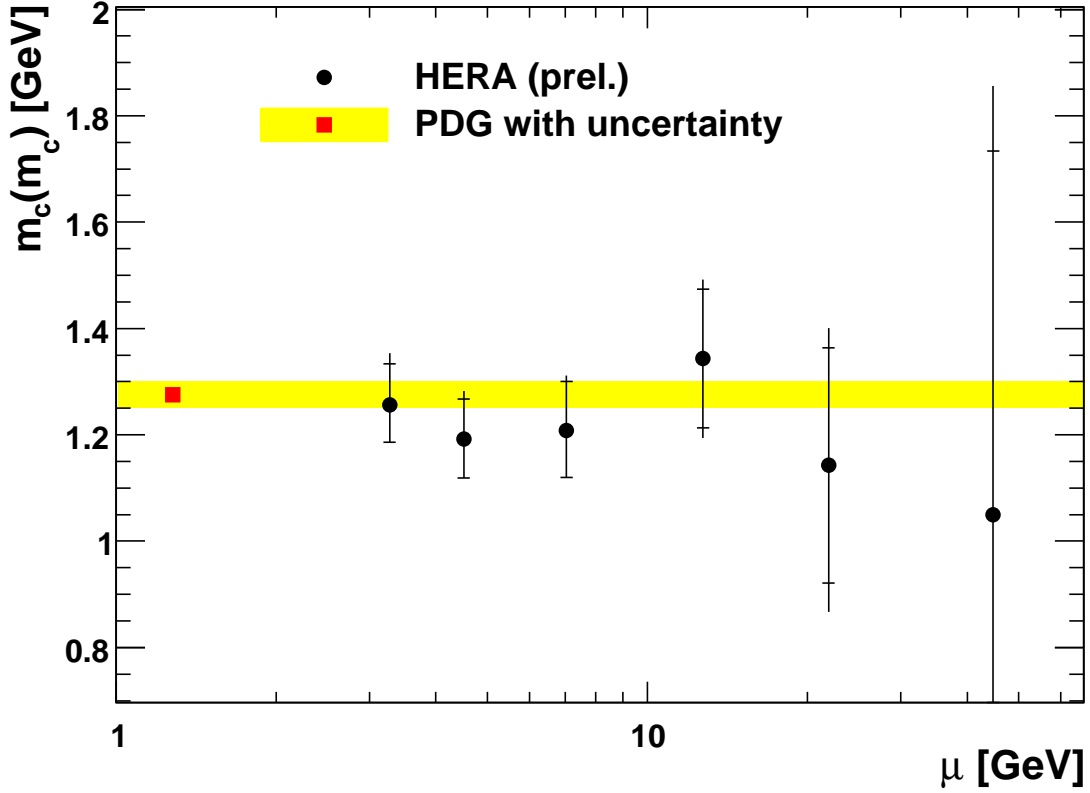


Figure 3: Measured charm mass $m_c(m_c)$ in the $\overline{\text{MS}}$ running mass scheme obtained independently from the six different Q^2 subsets of Fig. 1 (black points). Each result is displayed at a scale $\mu = \sqrt{\langle Q^2 \rangle + 4m_c(m_c)^2}$, where $\langle Q^2 \rangle$ is the logarithmic average Q^2 of the subset. The outer error bars show the fit uncertainty and the model, parametrisation [6] and theoretical systematic uncertainties (section 3) added in quadrature. The inner error bars show the same uncertainties excluding the uncertainties arising from the variation of the QCD renormalisation and factorisation scales. The red point at scale m_c and the associated band is the PDG world average [13].

H1 and ZEUS preliminary

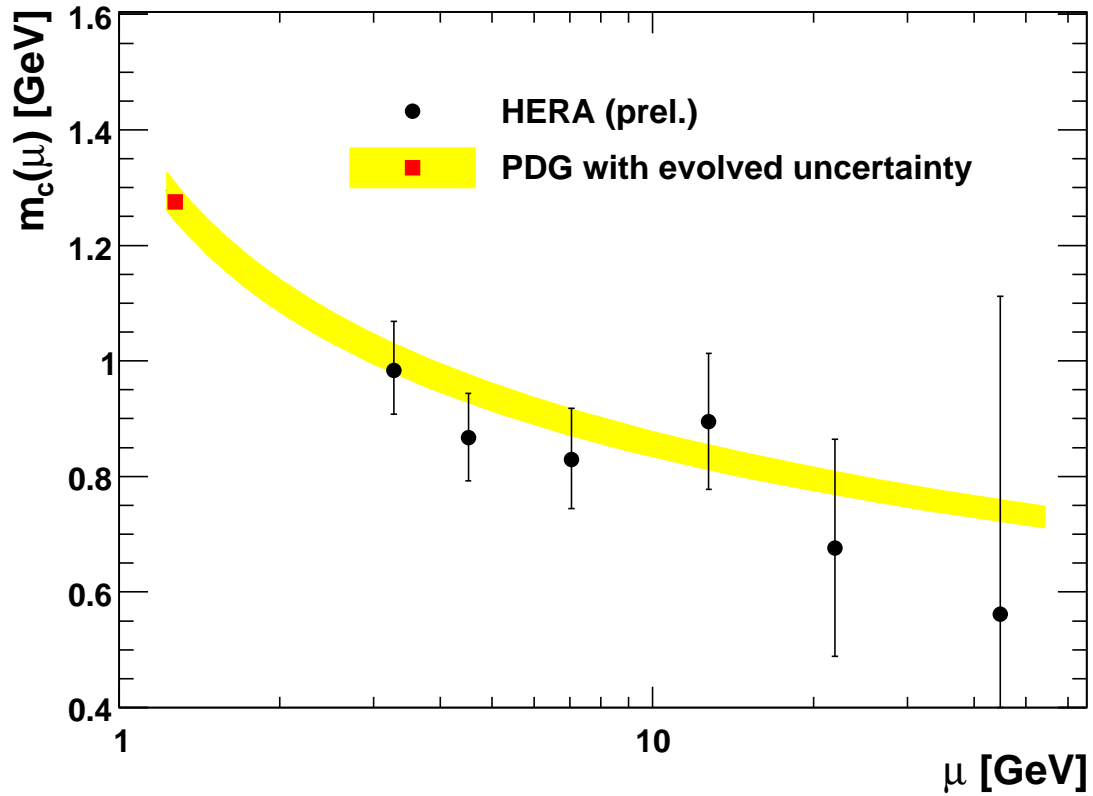


Figure 4: Measured charm mass $m_c(\mu)$ in the $\overline{\text{MS}}$ running mass scheme as a function of the scale μ as defined in Fig. 3 (black points). The error bars correspond to the inner error bars shown in Fig. 3. The red point at scale m_c is the PDG world average [13] and the band is its expected running [12]. The data are consistent with this running.